



Article

Morphometric Analysis of Pluto's Impact Craters

Caio Vidaurre Nassif Villaça ¹, Alvaro Penteado Crósta ^{1,*} and Carlos Henrique Grohmann ²

¹ Institute of Geosciences, State University of Campinas, R. Carlos Gomes 250, Campinas 13083-855, Brazil; c227996@dac.unicamp.br

² Institute of Energy and Environment, University of São Paulo, Av.Prof. Luciano Gualberto 1289, São Paulo 05508-010, Brazil; guano@usp.br

* Correspondence: crosta@unicamp.br

Abstract: The scope of this work is to carry out a morphometric analysis of Pluto's impact craters. A global Pluto digital elevation model (DEM) with a resolution of 300 m/px, created from stereoscopic pairs obtained by the New Horizons Mission, was used to extract the morphometric data of craters. Pluto's surface was divided according to different morphometric characteristics in order to analyze possible differences in the impact dynamics and modification rate in each region. A Python code was developed, within the QGIS 3× software environment, to automate the process of crater outlining and collection of morphometric data: diameter (D), depth (d), depth variation, slope of the inner wall (Sw), diameter of the base (Db), and the width of the wall (Ww). Data have been successfully obtained for 237 impact craters on five distinct terrains over the west side of Sputnik Planitia on Pluto. With the collected data, it was possible to observe that craters near the equator (areas 3 and 4) are deeper than craters above 35°N (areas 1 and 2). Craters on the western regions (areas 2 and 3) contain the lowest depth values for a given diameter. The transition diameter from simple to complex crater morphology was found to change throughout the areas of study. Craters within areas 1 and 4 exhibit a transition diameter (Dt) of approximately 10 km, while Dt for craters within areas 3 and 5 the transitions occurs at 15 km approximately. The presence of volatile ices in the north and north-west regions may be the reason for the difference of morphometry between these two terrains of Pluto. Two hypotheses are presented to explain these differences: (1) The presence of volatile ices can affect the formation of craters by making the target surface weaker and more susceptible to major changes (e.g., mass waste and collapse of the walls) during the formation process until its final stage; (2) The high concentration of volatiles can affect the depth of the craters by atmospheric decantation, considering that these elements undergo seasonal decantation and sublimation cycles.

Keywords: New Horizons; Pluto; impact crater; morphometry



Citation: Villaça, C.V.N.; Crósta, A.P.; Grohmann, C.H. Morphometric Analysis of Pluto's Impact Craters. *Remote Sens.* **2021**, *13*, 377. <https://doi.org/10.3390/rs13030377>

Received: 17 November 2020

Accepted: 15 January 2021

Published: 22 January 2021

Publisher's Note: MDPI stays neutral with regard to jurisdictional claims in published maps and institutional affiliations.



Copyright: © 2021 by the authors. Licensee MDPI, Basel, Switzerland. This article is an open access article distributed under the terms and conditions of the Creative Commons Attribution (CC BY) license (<https://creativecommons.org/licenses/by/4.0/>).

1. Introduction

Impact cratering is an active and fundamental phenomenon from the initial accretion of bodies on the protoplanetary disk to the present day. It is the main process by which planetary surfaces are modified. Morphometric data of impact craters are fundamental for understanding the evolution of the Solar System and its components [1]. The study of impact craters can result in a vast amount of information, such as the ages, rheology properties, erosion rate of planetary surfaces, as well as constrain the cratering history (impact flux) on terrestrial planets and other solid planetary bodies [2].

Robbins et al. [3] reviewed the main methods for morphometric analysis of impact craters using remote sensing data. Since digital elevation models (DEMs) allow the analysis of these structures in three dimensions, Robbins et al. [3] favor the use of DEMs to obtain morphometric data. Robbins and Hynes [4] analyzed the morphometry of Mars' impact craters in order to determine the planet's global and regional transition diameter (Dt). Dt represents the threshold that defines the formation of simple craters (formed below Dt) and complex craters (formed above Dt). This transition between simple and complex

craters occurs due to a change in the regime that predominates in the process of crater formation [5]. Robbins and Hynes [4] found that, near Mars' equatorial region ($Dt = 6$ km), the craters are deeper than those near the poles ($Dt = 11$ km), probably due to the presence of volatile elements. Watters et al. [6] observed that Martian craters that were formed in regions of more resistant rheology (e.g., basalt) are deeper than craters formed in weaker material (e.g., ejecta deposits).

In July 2015, the New Horizons spacecraft imaged approximately 30% of Pluto's surface [7]. Since then, some preliminary studies regarding the morphometry of its impact craters have been carried out, and the subject needs to be further investigated. According to Moore et al. [8], the New Horizons mission found out that Pluto's surface is mainly composed of H_2O , CH_4 , CO , and N_2 ices. The dwarf planet has active geological processes and atmospheric cycles which still modify its surface in the present. Robbins et al. [9] identified approximately 5200 circular structures on Pluto's surface and divided them into a five-point scale system, where one means little chance of being an impact crater and five indicates a certain impact crater. Robbins et al. [9] measured the diameter of each impact crater on Pluto to create a global distribution of impact frequency by size. A preliminary division of Pluto's surface into morphological domains was presented by Moore et al. [8]. Robbins et al. [10] measured the depth and diameter of 113 craters on Pluto's surface and deduced a global transition diameter of approximately 10 km.

Singer et al. [7] observed a deficit of small craters (less than 15 km) over the entire surface of the dwarf planet by analyzing their size frequency distribution (SFD). As it would be unlikely that the possible processes of erosion and modification present in icy bodies could modify only small craters, this observation may also reflect the deficit of small objects in the Kuiper belt. It is still necessary to analyze in more detail the morphometry of Pluto's impact craters in order to help decipher their formation dynamics and the processes that could modify them throughout the dwarf planet's surface.

Since Pluto exhibits a complex geology (Figure 1), the scope of this work is to carry out a detailed analysis of the morphometry of the impact craters larger than 5 km and up to 60 km in diameter, within different terrains across Pluto's surface. This is intended to assess if there is any correlation between the differences of morphometry and the different compositions of Pluto's surface. In addition, we investigate the transition diameter between simple and complex craters of Pluto in these different terrains.

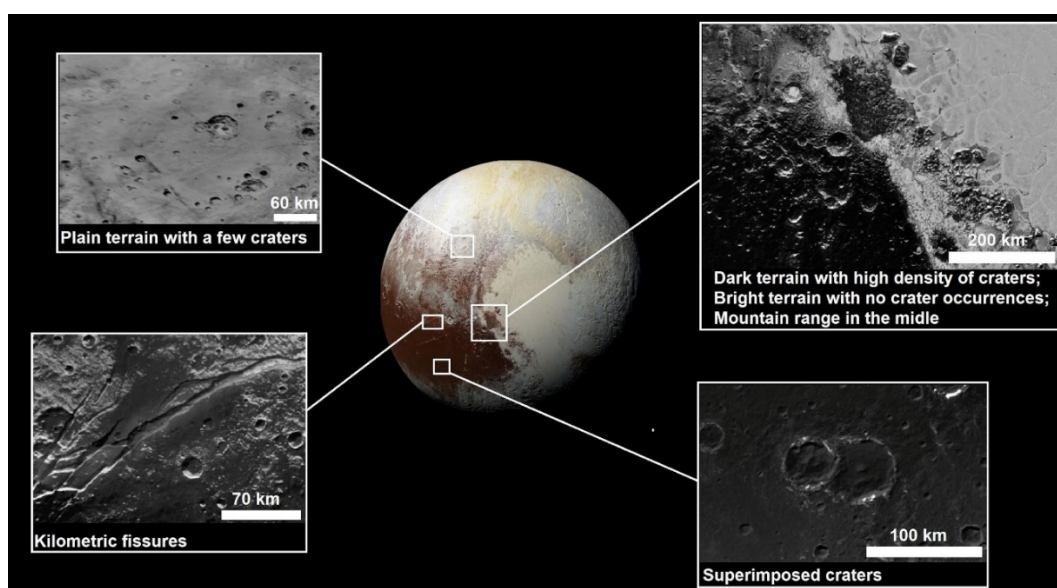


Figure 1. Global view of Pluto obtained by the combination of blue, red and infrared images taken by the Ralph/Multispectral Visual Imaging Camera (MVIC) (Image modified from Moore et al. [8] and Schenk et al. [11]; www.solarsystem.nasa.gov).

2. Materials and Methods

2.1. Study Area

Pluto, currently designated as a dwarf planet, is 5.9 billion kilometers from the Sun and is the main object of the Kuiper Belt. The study area comprises the region west of Sputnik Planitia (SP), between 0° and 180° longitude (Figure 2). In this area, images with the best spatial resolution acquired by New Horizons are found in a variety of morphologically distinct domains containing the majority of impact structures of Pluto's surface [7,9].

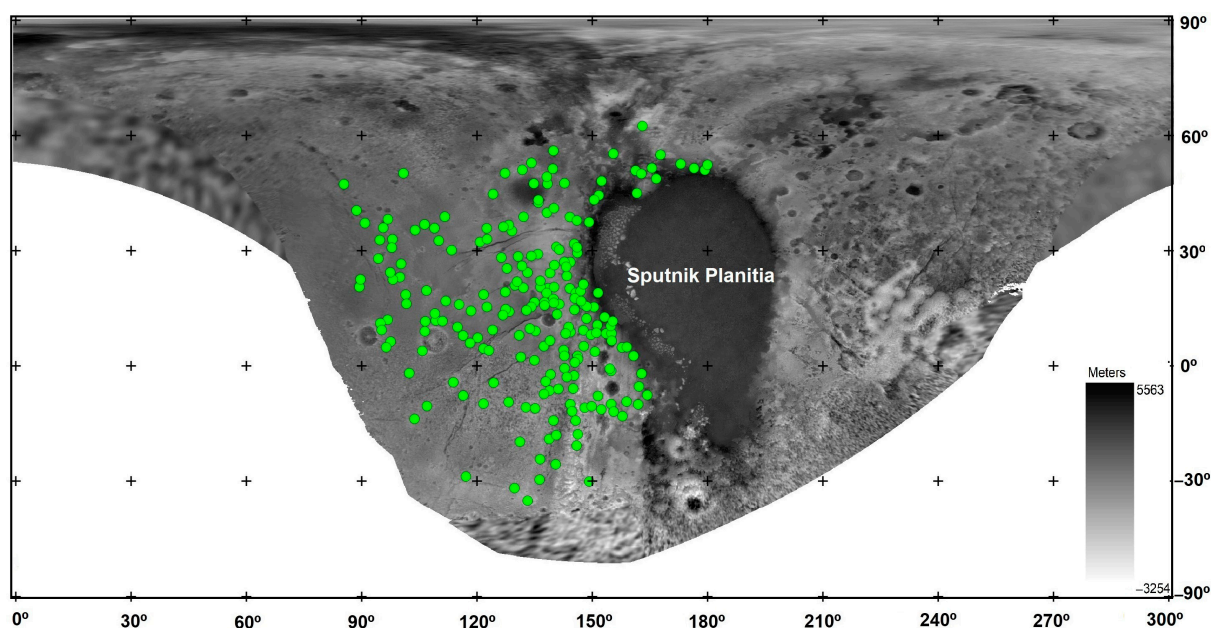


Figure 2. DEM of Pluto's surface [8,11]. Dots represent the 237 craters analyzed in this work (Table S1).

Pluto's surface is composed mainly of H₂O, CH₄, N₂, and CO ices [8]. H₂O ice is known to be a strong material, capable of forming mountains with high slopes [8]. N₂, CO, and CH₄ ices are all volatile elements at Pluto's surface temperatures of 35 to 50 K [12]. According to these authors, N₂ is the most volatile ice in the surface of Pluto and is concentrated mostly above 30°N. North-west regions have the presence of bright halo craters, which have a dark base and a high albedo edge, probably composed of methane (CH₄). Pluto has a variety of exogenic and endogenic processes that modify its surface: viscous relaxation, tectonic processes, mass waste, glacial erosion by the flow of volatile ice, precipitation of particles from the atmosphere, erosion by sublimation, subsurface convection activity, and cryovolcanism [7,8,12].

2.2. Morphometric Analysis

In view of the wide variety of methods for outlining impact craters, this study uses as a basis the method developed by Geiger [13]. A Python code was developed (see supplementary material) in order to automate the outlining step of impact craters and create a systematic method that can be easily replicated. The code works in the QGIS 3x software environment [14]. It was used to outline 237 craters (Table S1). We have considered successful outlines the ones with minimum visual errors (Figure 3A). The largest errors occurred in very uneven terrains (Figure 3B), where the pre-impact topography influences the analysis. Because the analysis conducted in this work covers the average values for each morphometric feature, small errors should not strongly influence the final results. The code calculates the following morphometric data: diameter (D), depth (d), depth variation, slope of the inner wall (Sw), diameter of the base (Db), and the width of the wall (Ww) (Figure 3C). It also calculates the standard deviation of each value and extracts the coordinates of each crater.

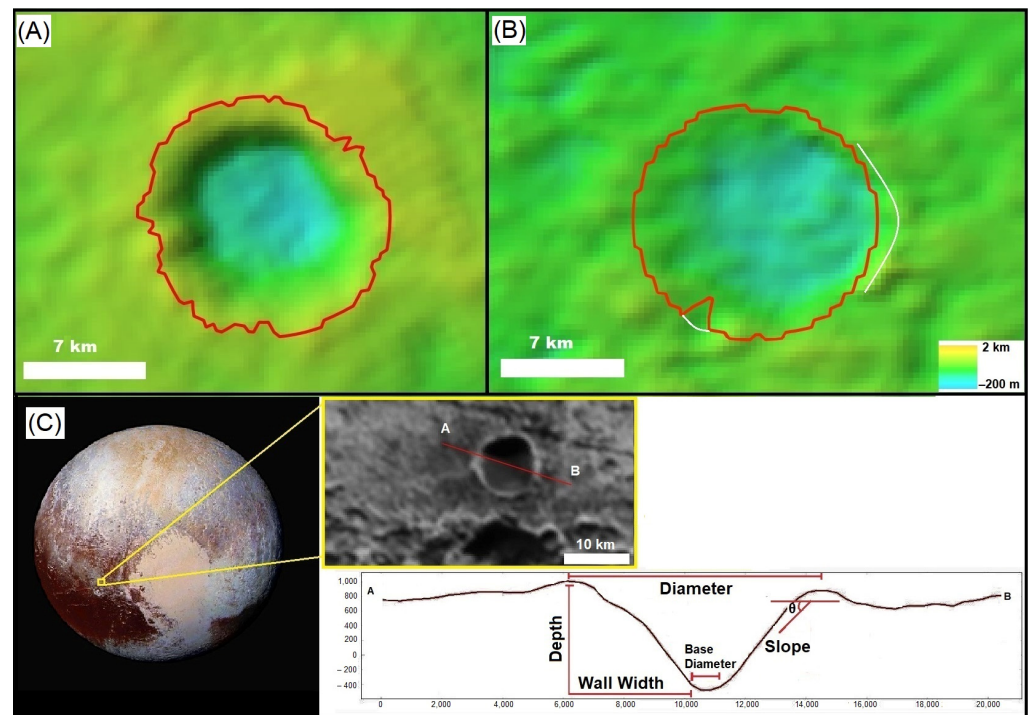


Figure 3. (A) Crater with a good outline. (B) Crater with some outline errors and, therefore, excluded from further analysis. The red lines represent the outlines processed by the Python code for two different craters, each one with different levels of success. White lines represent the ideal outline. (C) Profile of a simple crater on Pluto's surface showing the data extracted by the Python code.

From an initial approximate circle, defined interactively by the user, the code analyses as many profiles as the resolution of the DEM allows. The profiles are $1.3\times$ longer than the fit circle radius in order to increase the chances of the profile encompassing the crater rim. The code first searches for the point of maximum elevation (ME) of an initial profile, then it checks if the ME of the next profile is within a determined radius of the initial ME. If not, a control point in the middle of the first ME and the second ME is selected. The ME points are searched within a determined radius in order to reduce the chances of the code selecting a ME that represents a pre-impact terrain, and not the crater rim. The depth of the structure is calculated by: (point of lowest elevation of the base of the crater) – (value of the average height of the crater wall). More details about the code are explained in the supplementary material.

In order to eliminate projection errors, each crater is reprojected as the center of a stereographic projection, before having their morphometric data extracted by the code. Uncertainties in diameter and depth measurements are calculated according to Robbins et al. [10].

2.3. Modification and Morphologies

According to Bray and Schenk [15], Pluto must have a large spectrum of well-preserved craters with different morphometric features, due to the relative low speed of impacts against its surface. Bray and Schenk [15] show that craters formed by impacts with velocities greater or smaller than 2 km/s are shallower than craters formed by impacts with this velocity. This makes the modification rate analysis qualitative rather than quantitative, since it is not possible to know if the different morphometry is caused by erosion and modification, or by differences in impact velocity. There are several factors that can modify an impact crater on Pluto: decantation of material suspended in the atmosphere, viscous ice relaxation, tectonics, mass movement, glacial erosion, cryovolcanism, sublimation, filling, and superimposition of craters [7].

In order to remove the influence of anomalous morphometries, as much as possible, craters with an advanced stage of modification were not considered in the analysis. The modification states of the craters analyzed in this work were defined based on two methods: visual analysis of the images and selection of the deepest craters for each region.

The visual analysis of the global panchromatic mosaic of Pluto was complemented with the evaluation of the profiles generated by the algorithm created in this work. We classified, qualitatively, the degree of preservation of the crater shape using the profiles and checking for eventually superimposed craters that could influence the depth of the crater. This analysis can determine whether the craters appear to be modified or not (Figure 4). Craters are considered deformed if the asymmetry between rim high and slope of inner walls are too high, as shown in Figure 4C. In some cases, the superimposed crater modifies the rim, or creates a false notion of increased depth if located inside the crater being analyzed.

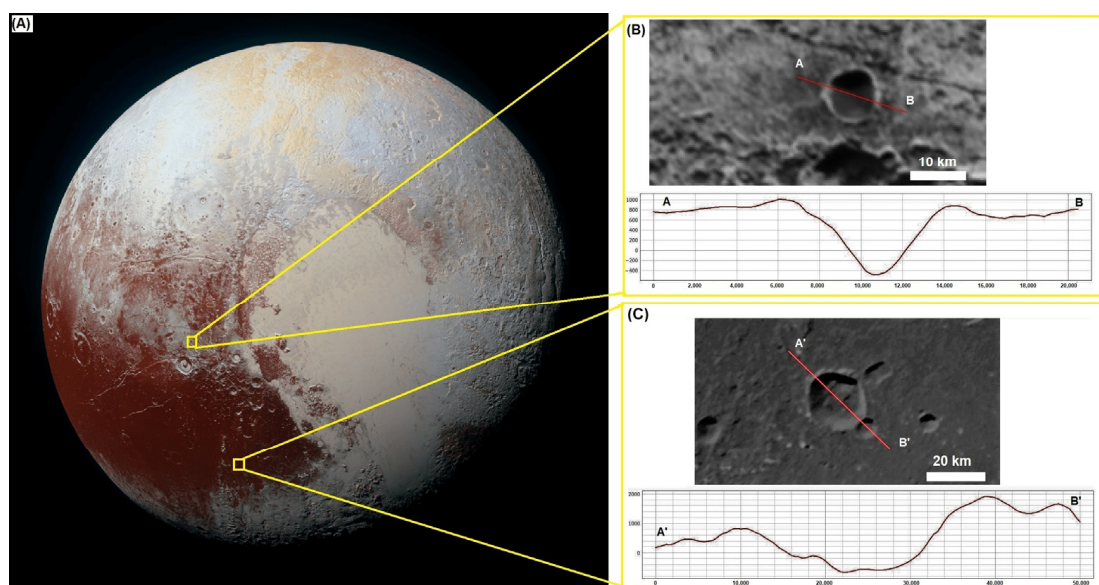


Figure 4. (A) Global view of Pluto. The image combines blue, red and infrared images taken by the Ralph/Multispectral Visual Imaging Camera (MVIC) (Credits: NASA). Profiles x and y axis are in meters. (B) Well preserved simple impact crater. (C) Simple crater with a high level of modification: internal walls with low slope; surrounding craters modify its morphology; rim with uneven height.

The second method to determine the modification rate of craters is the selection of the deepest craters within the same region on Pluto's surface. This method is based on the concept that the deepest craters, within the same rheological material and the same diameter range, are the freshest ones, since they might be the least modified by the main modification processes (infilling or ice relaxation) [4]. Consequently, two datasets are created, one with all craters and the other with only the freshest ones. Craters anomalously deep are removed from the dataset, so it is possible to reduce the chances of factors such as superimposed craters influencing the analysis of the crater's depth. Anomalously deep craters are the ones that exhibit a large depth for its diameter and do not follow the trend of the majority of the craters [3].

The classification of the basic shape of the crater was done manually, observing the profiles extracted by the Python code. Complex craters can be identified by the presence of a central peak, walls containing terraces and a flat base. In the case of filling, the central peak can be buried, so the classification is based mainly on the shape of the base. Simple craters have a more pronounced bowl shape.

The dataset was separated into groups of regions and diameters. This separation is necessary to avoid misinterpretation of the data, since craters in different areas throughout

Pluto's surface may contain different primary morphometries, in addition to undergoing different processes of erosion and modification. According to Robbins and Hynek [4], it is important that the deepest crater analysis be separated into regions, since different regions may have fresh craters of the same diameter with different depths due to the composition of the superficial crust. Thus, if the analysis is not done separately for each region, the ones containing shallower craters by nature could always be interpreted as more modified than the others.

3. Results

Figure 5 shows the d/D ratios of the freshest craters versus their location in latitude and longitude. It is noteworthy that the northernmost craters have lower d/D ratios than the others. It is also possible to observe that the southernmost craters do not have depths as shallow as the equatorial and northern craters that reach the lower limit of the d/D ratio. Craters near the equatorial regions show great variability in the data, going from the lowest d/D of 0.04 to the highest d/D ratio value > 0.20 (Figure 5A). In the plot that relates the d/D ratio to the longitude (Figure 5B), we can see that craters located between 150° and 120° have higher d/D ratios than craters to the west ($<120^\circ$). Western regions exhibit the lowest values of d/D ratios (Figure 5B). Figure 6A shows a heatmap separating the craters in bins of 100 km^2 (bins with no craters are not considered). Figure 6A clearly shows that northwestern areas tend to have lower d/D ratios than southeastern ones, and that craters near the equator have the highest for d/D ratios and variability.

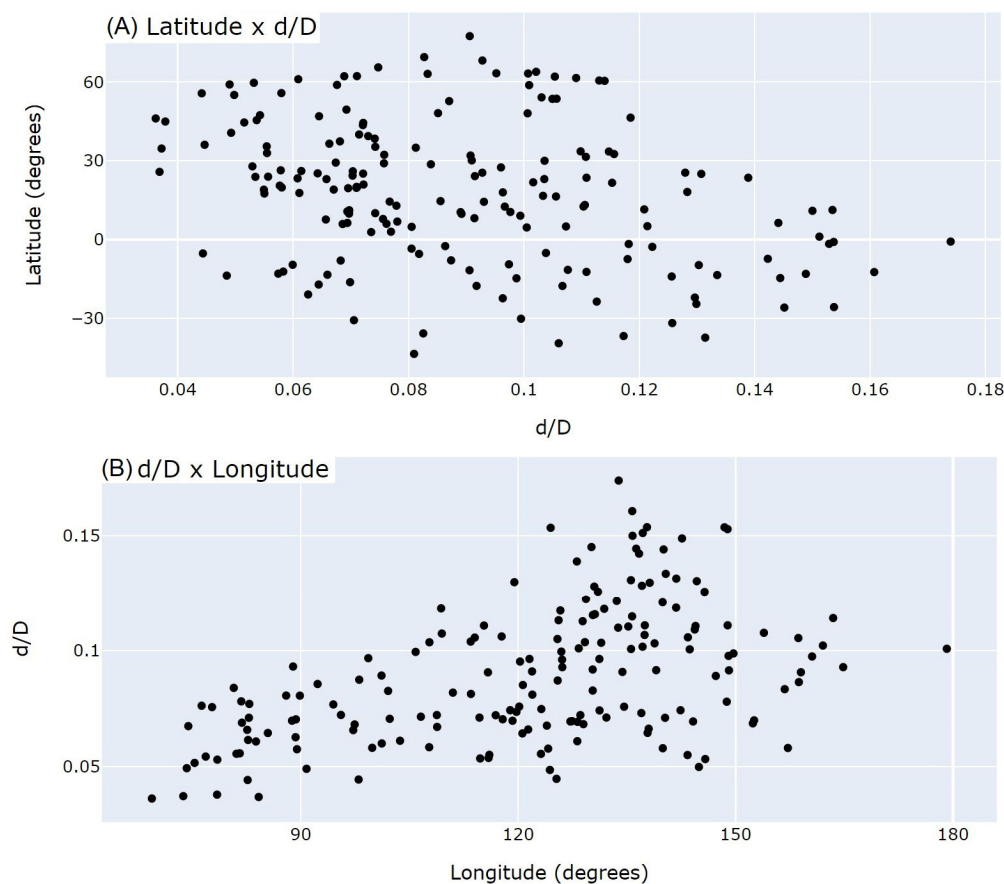


Figure 5. d/D ratios related only to freshest craters plotted according to: (A) latitude; (B) longitude.

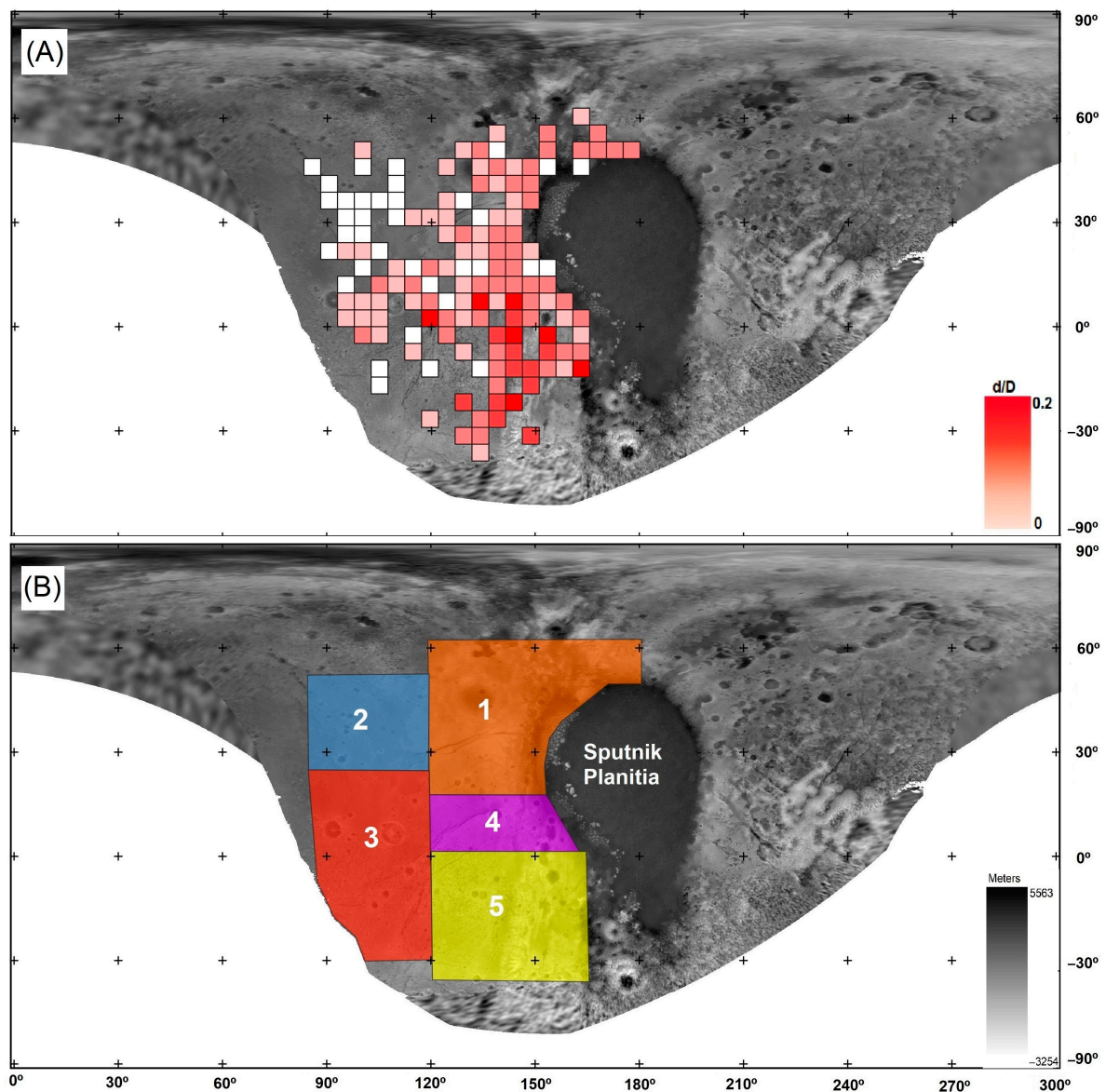


Figure 6. (A) Heatmap showing bins of 100 km² with mean values of d/D ratios. Bins with no craters are not considered. (B) Areas dividing Pluto's surface into five groups.

In order to better understand the variability of morphometry across Pluto's surface, areas of common d/D patterns were grouped together, using Figures 5 and 6, in five different regions (Figure 6B).

Craters within areas 2 and 3 (i.e., craters within the western – northwestern regions) tend to be shallower than the craters in eastern terrains. Areas 4 and 5 contain the deepest craters of our database comparing structures of the same diameter. Area 1 groups together craters of medium to low d/D values.

Figure 7A shows the measured values of depth and diameter for the freshest measured craters of all areas, while Figure 7B–F show the same data, but considering separately simple and complex craters within each morphological domain. Craters of areas 1 and 4 show a change of slope trend of the graph approximately in 10 km of diameter (Figure 7B,E). Craters within Area 3 and 5 (Figure 7D,F) show a change of trend in ~15 km of diameter. The lack of small craters (<12 km) in area 2 limits the comparison between this area and the others, but is possible to notice that the data collected in it shows that craters <12 km are considerable shallower than craters larger than 15 km.

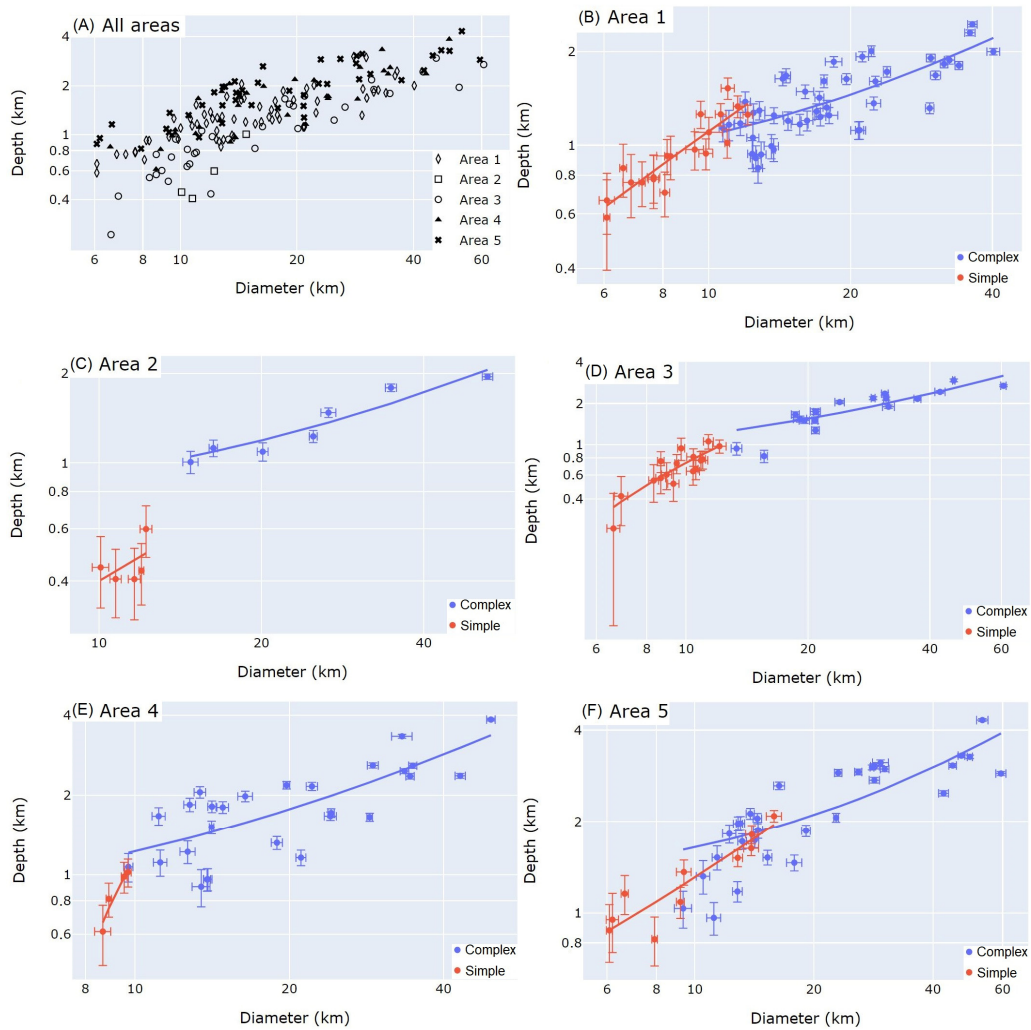


Figure 7. Depth vs Diameter plotted on log–log scale. Only the freshest craters of each area are considered. Data are divided into simple and complex structures. (A) all areas. (B) area 1 (C) area 2. (D) Area 3. (E) Area 4. (F) Area 5.

Figure 8, representing only the freshest craters, shows that craters over 15–20 km in diameter tend to have a smaller d/D ratio in comparison to craters with smaller diameters (<10 km). Also, craters smaller than 15 km of diameter within near equatorial westerns regions (area 4 and some craters of area 5) reach higher depth/diameter ratios ($d/D > 0.1$) compared to crater within northern-northwestern regions.

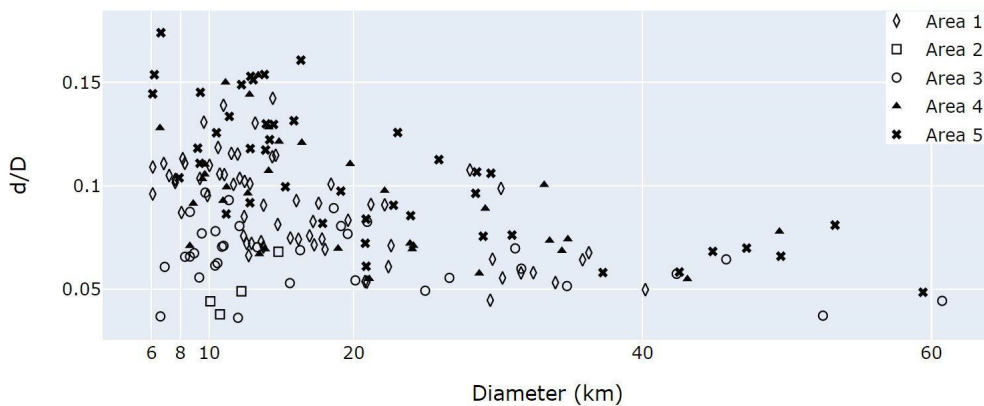


Figure 8. d/D ratio vs Diameter plot of freshest craters only. Note that Area 2 and Area 3 terrains are predominant at the bottom of the plot.

Assuming that the observed width and slope of the internal wall of the impact craters should increase as the craters undergo erosion and filling processes, Figure 9 relates wall width (W_w) with depth of the freshest craters of each area. It shows that craters of areas 4 and 5 tend to remain in the lower values of the plot. Other areas show a similar diversity of ranges for each depth value.

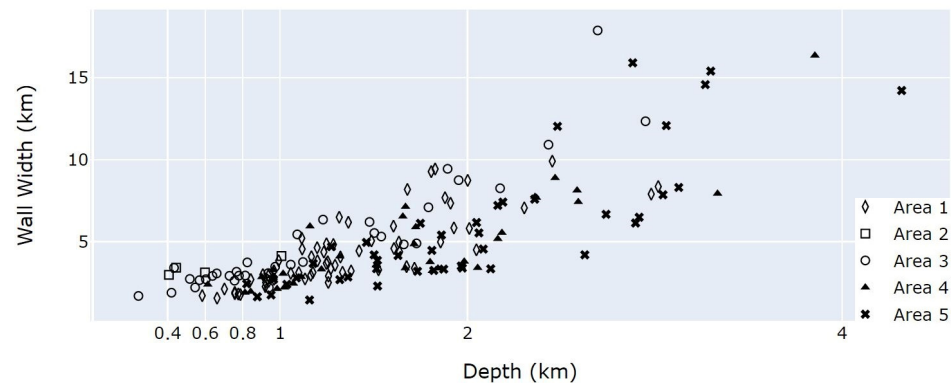


Figure 9. Wall width (W_w) versus depth of the freshest impact craters.

In Figure 10, the depth variation (standard deviation of the rim-floor depths extracted in all profiles of a crater) of all craters is plotted against diameter (Figure 10A) and depth (Figure 10B). There is a positive correlation of increasing diameter and depth as depth variation increases.

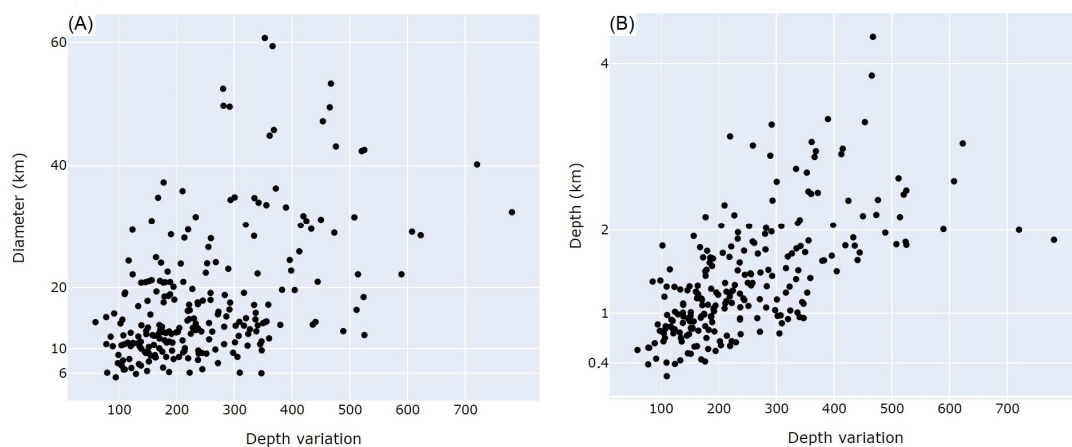


Figure 10. (A) diameter versus depth variation of all craters. (B) Depth versus depth variation of all craters. All craters plotted.

Figure 11 shows the relation of the slope of the inner wall (S_w) with diameter. Most of the craters are concentrated between 10 and 20 degrees of slope of the inner wall. Between 10 and 15 km in diameter there is a considerable presence of craters from areas 4 and 5 on higher slope values. Craters within areas 2 and 3, on the other hand, are concentrated in general in the areas of lower declivity of inner walls. Figure 12A shows a tendency of increasing S_w with depth. As we plot all craters in Figure 12A, it is possible to observe a higher spread of data as slope and depth values increase. To better understand this data spread, three different trends were defined in the chart (see Section 4 “Discussion”). Figure 12B shows a strong linear correlation of S_w and d/D ratios for all craters. The tendency of increasing S_w with depth is better observed when plotting only craters of the same diameter (10–11 km in Figure 12B).

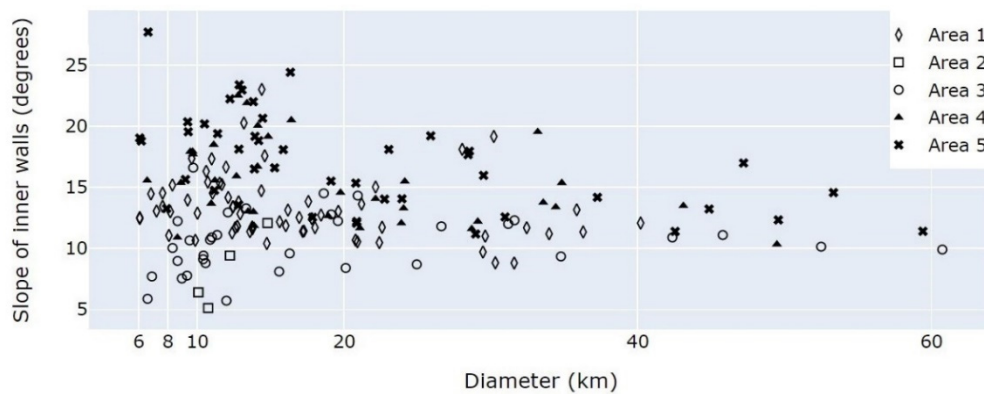


Figure 11. Slope of inner walls (S_w) versus diameter of impact craters. All craters plotted.

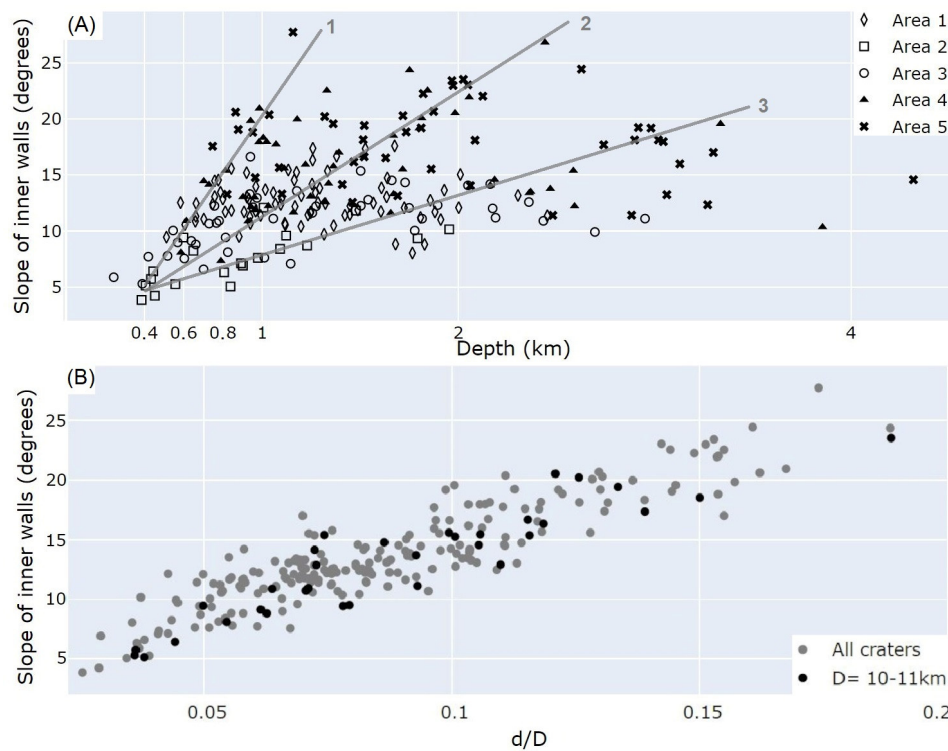


Figure 12. (A): slope of inner walls (S_w) versus depth. Lines indicate three different apparent data trends (All craters plotted). (B): S_w vs d/D ratios for all craters (gray) and for craters with diameter between 10 and 11 km (black).

Figure 13 shows the relation of depth and the depth variation for a diameter of approximately 10 km. The plot shows a positive linear correlation between the two morphometrics variables. There are three points with large discrepancies (near 1 km depth).

Figure 14A,B show a strong linear correlation of wall width (W_w) and base diameter (D_b) with diameter (D). Both plots show data spreading at 20 km of diameter.

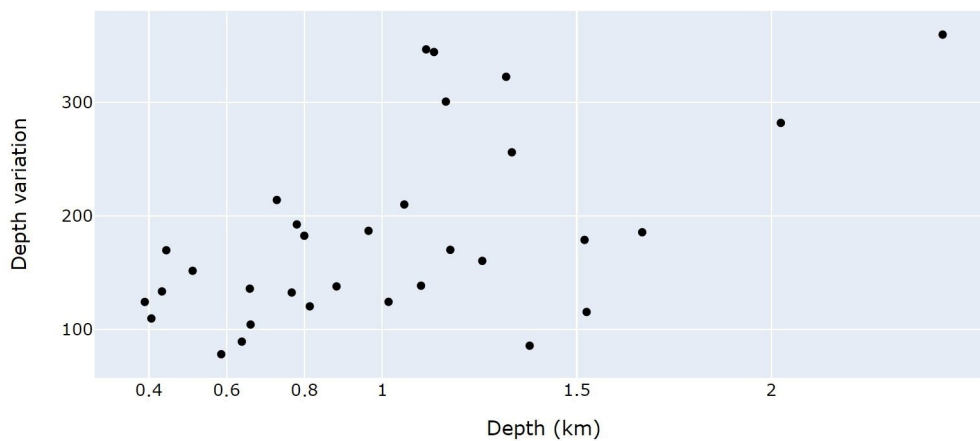


Figure 13. Depth versus depth variation. Data plotted is strictly for craters with approximately 10 km of diameter.

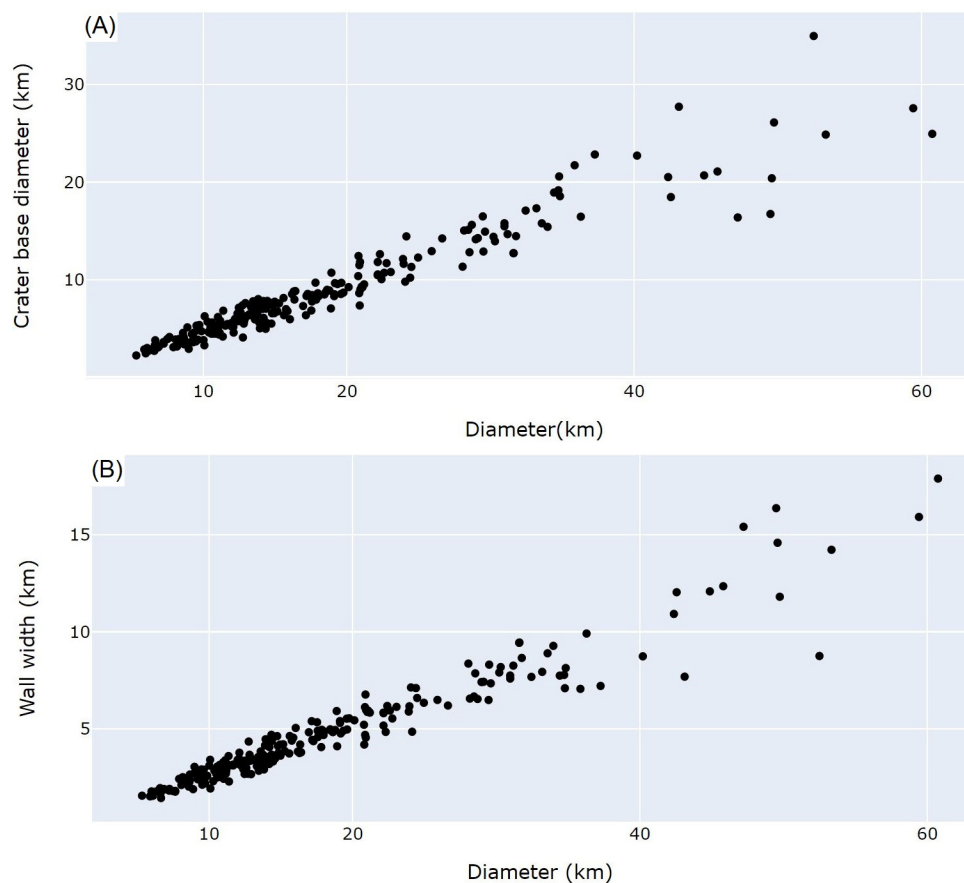


Figure 14. (A) Wall width versus diameter. (B) Diameter of base versus Diameter. All craters plotted.

4. Discussion

4.1. Transition Diameter

Schenk et al. [11] and Schenk [16], each applying different methods, concluded that the transition diameter between simple and complex craters for Pluto are 4.3 km and 10 km in diameter, respectively. The transition diameter is inversely proportional to the gravity of the body [17]. Knowing that the gravity of Galilean satellites is approximately twice that of Pluto, the transition diameter on Pluto is expected to be twice that on Galilean satellites. In addition, the impact speed on Galilean satellites is approximately 23 km/s [15], whereas on Pluto it is 2 km/s [18]. Therefore, deeper craters are expected to form on Pluto

as calculated by Bray and Schenk [15]. Knowing this, a higher d/D ratio for the dwarf planet in comparison with the Galilean satellites is predictable.

Comparing the data for Galilean satellites of Schenk [19] and the results from this study, it is possible to confirm that craters on Pluto are indeed deeper. For example, a crater with 20 km of diameter has a depth of 1 km on Galileans satellites and 2 km on Pluto. Iapetus and Rhea have a lower gravitational acceleration than Pluto, thus, the transition diameter of Pluto must be an intermediate value in between these bodies. The body with gravitational acceleration closest to Pluto is Triton, which has a transition diameter of approximately 11 km in diameter [20].

Schenk et al. [11] measured the diameter and depth of only complex craters on Pluto's surface and used a d/D ratio of 0.2 for unmodified simple craters. Schenk et al. [11] indicated a simple to complex transition diameter of ~4.3 km, as expected from the extrapolation of the other icy bodies. Due to the fact that only craters larger than 5 km of diameter were computed in this work, it is not possible to verify the transition diameter proposed by Schenk et al. [11]. However, it is possible to observe a slope change at 10 km, therefore a transition diameter for simple to complex craters of 10 km in areas 1 and 4, as expected based on the calculations of Schenk [16] and Robbins et al. [10]. Areas 3 and 5 show a slope change at approximately 15 km of diameter. Robbins et al. [10] found a transition diameter (D_t) of 10 km for Pluto but, without dividing it in different terrains, it was not possible to observe a different D_t for different regions as reported here. Robbins et al. [10] interpreted that a higher proportion of rocks in Pluto's crust could explain the fact that the D_t in the dwarf planet is higher than expected from the extrapolation of the D_t from other icy bodies. So, a basic interpretation of the areas with D_t ~15km found in this work could be that, in these areas, the crust could contain a higher percentage of rocky materials mixed with ice in comparison to the rest of Pluto. Also, visual analysis was conducted to separate complex craters from simple craters mainly using the following features: flat base (complex) and parabolic base (simple), and presence or absence of a central peak. It is possible to observe craters up to a maximum of ~16 km of diameter with features compatible with simple craters. Other craters with at least ~9 km of diameter contain features compatible with complex structures. This indicates that the transition diameter may be in the range between 9 and 16 km.

4.2. Morphometric Differences

Taking into account the analysis of deeper craters to define the freshest structures (Figure 5A), craters at latitude close to 0° and longitude between 150° and 120° have the highest variation of depths for a given diameter, which could indicate a variability in modification rates in these areas. It is noteworthy that the analysis of the deepest craters, within the same area and the same diameter range, indicates the least modified ones. However, in a few cases, some craters in the group of the deepest ones may have been modified by overlapping craters, which can artificially increase their depth. Visual analysis shows only a few cases of overlapping craters, so the method of deepest craters appears to be efficient for statistical analysis.

Considering only the western region of Sputnik Planitia (SP), where data were collected for this work, the craters located between longitude 150° and 120° and latitude 15° and -30° have higher d/D ratios than the westernmost craters (longitude $< 120^\circ$) and northernmost craters (latitude $> 30^\circ$). Since craters located within areas 4 and 5 are usually the deepest craters of Pluto for almost every diameter (analyzing the freshest craters only), this could explain the higher d/D ratios of these areas (Figure 6). As the DEM available for Pluto does not cover latitudes beyond -30° (Figure 2), it impairs the analysis if there are differences between morphometries in low latitudes, as those that we can find in higher latitudes.

Singer et al. [7] estimated that the whole western part of Sputnik Planitia is very old and has approximately the same age. Therefore, it is impractical to associate the morphometry difference with the age of the dwarf planet's surface. However, we can

associate the morphometric differences between northern and equatorial/southern regions with a higher rate of modification. Low depths in the northern-northwestern regions may be due to sublimation of volatiles (discussed below). A constant deposition during the different seasons of Pluto could also end up eroding and modifying the craters in a more intense way in the northern-northwestern regions, compared to the equatorial regions [12].

As the lower limit of d/D ratio in almost all longitude ranges is similar (Figure 5B), the difference in d/D ratio between them does not necessarily indicate the western part has undergone greater modification. Rather, the newly formed craters further to the west could be shallower compared to craters of the same diameter in the eastern regions. On the other hand, Figure 5A shows that the lower limit of d/D values increases from north to south, which could indicate a lower degree of modification towards lower latitudes. Yet, another hypothesis would be that the modification processes in the northwestern region (mainly area 2) could be sufficient to erode a larger number of craters and eliminate craters with higher d/D values, compared to the equatorial regions that concentrate craters with a wide range of d/D values. The spatial location of the equatorial craters exhibiting a great variability in d/D ratios is concentrated in a restricted area of Pluto, and not randomly placed throughout its surface, reinforcing the idea that these craters were formed in a region with similar rheology.

Comparing the regions with the highest d/D values, it is possible to observe differences in morphometry. Simple craters in area 5 are deeper than craters in area 4. Knowing that deepest craters should represent the least modified structures, the difference in depth could represent a different modification state between equatorial and southern craters.

Larger craters tend to be formed earlier in the Solar System, so they accumulate more superimposed impacts and are affected by deformation processes for a longer period of time. On the other hand, smaller craters are more susceptible to these changes, so rim degradation and infilling by wall collapse would be more effective in reducing the d/D ratios of smaller craters (shallow ones) than the large (deeper) ones [21]. This pattern is shown in Figure 8, which depicts that craters with 10 km or less of diameter (taking into account the same terrain) have a greater range in the d/D ratio, which may indicate a higher rate of modification for craters in this size range. Figure 11 shows that smaller diameter craters tend to have a greater slope variability, which may show that the smaller the craters are, the more affected by filling or mass waste they are, factors that can decrease the slope of the wall. Larger craters do not appear to be so susceptible to decreases in the crater's slope, which agrees with the work by White et al. [21].

Craters of the same age and region, within the same diameter range, should have the same depth and other morphometric aspects. When separating the data of the plot showing slope vs d/D in craters with diameters between 10 and 12 km (Figure 12B), it is possible to observe that the shallower the crater is, the lower is the slope of the inner wall. According to Figure 12B, craters with lower d/D ratios in the same region have lower slopes in the inner walls. It is possible to assume that the more modified a crater is, the lower the slope angle of the inner walls of the structure will be, perhaps due to mass wasting.

Considering that pristine craters across Pluto's surface have similar morphometry, Figure 12 shows three different trends that could indicate different levels of modification. The slope of the inner wall should decrease with increasing modification, then the trend #3 shown in Figure 12 may represent the most modified craters by infilling, mass waste or ice relaxation. In this figure it is possible to observe that the higher values (least modified craters) are dominated by craters within areas 4 and 5 (and some craters of area 1) and that craters within areas 2 and 3 are concentrated under 15° of slope (higher rates of modification). Figure 11 shows that craters larger than 15 km tend to decrease d/D ratios. When observing the plot using only craters smaller than 15 km, the ones that have a lower d/D ratio are craters that must have undergone more modification due to infilling or ice relaxation.

It is possible to verify a difference in trend for craters with diameter greater than 20 km in different figures in this work (Figure 11, and Figure 14A,B). Figure 11 shows that

craters over 20 km of diameter exhibit a smaller slope. Figure 14A,B show that craters larger than 20 km tend to present more spread data. This observation may be an indication of ice relaxation, since this process generally affects larger craters [7,21,22].

Crater of the same age with low depths within the same morphological terrain and same diameter might indicate high levels of modification. The pattern of Figure 13 may mean that the smaller depth variation represents the most deformed craters, since erosion may have deformed the entire rim equally. On the other hand, well-preserved craters may have a high rate of standard deviation from the rim due to topography interference or may indicate that erosion have not yet degraded all the rim equally. This differs from what was previously thought, namely that high depth variation should represent high levels of modification of impact craters. The anomalous points in Figure 13 may represent those with higher levels of modification or terrain influence previously to the crater formation.

Robbins and Hynes [4] gathered an extensive database of Mars impact craters ≥ 1 km, and found that craters near equatorial regions are deeper than the ones in areas of high latitudes. The authors concluded that the volatiles present near the poles could melt during crater formation and fill the crater during the modification phase, therefore making them shallower. Figure 7A shows that the most pristine craters within areas 4 and 5 tend to be deeper for a given diameter than in the western-northwestern regions. These differences related to the deepest craters could represent a change in rheology between different regions of Pluto's surface, a suggestion presented by Robbins and Hynes [4] and Watters et al. [6]. As shown in Section 4.1, the different transition diameters found in each area could also be explained by the respective different proportions of ice and rock materials. Also, another hypothesis to explain the morphometric differences between regions on Pluto could be due to the presence of volatiles during the formation of the crater (during its modification stage), when the impact energy melts the volatiles that, subsequently, fill the crater [4].

According to Grundy et al. [12], there is evidence for mantling, or covering of a terrain with a new layer of material in Pluto's surface. This is most clearly observed in Pluto's northern areas, with the presence of N_2 , CO , and CH_4 ices, that are all volatile at surface temperatures of 35 to 50 K. Of the three compounds, N_2 has the highest vapor pressure and thus dominates the lower atmosphere [12]. Many craters in western regions above 0° of latitude, show strong CH_4 absorption on their rims but not on their floors [12]. N_2 absorption appears strongest on many crater floors, notably those in the northern regions, where partially filled larger craters are found, implying that smaller craters may be completely buried by mantling [7,12]. Since impacts on nitrogen layers above water generate deeper craters with smaller diameter [23], in the case of Pluto the lower d/D ratio for northern regions (which shows strong presence of N_2), could be due to the N_2 being responsible for infilling the craters by atmospheric deposition rather than being influenced during the impact process. This does not exclude the possibility that other volatiles are interfering with the formation of impact structures, turning shallower craters in the northern regions of Pluto. In the same way, the strong presence of volatile CH_4 in the craters' rim from areas 2 and 3 could also explain the low values for d/D in these regions, either influencing the crater formation or post-modifying it.

Visual analysis of the images does not allow to identify classes of modification rate in different regions, since the entire western part of Sputnik Planitia has a similar age and lack of well-preserved craters. Since the presence of volatile elements in the northern part of Pluto indicates greater levels of erosion rate, it is simpler to assume that the rate of erosion at higher latitudes is high. Therefore, the wide range of variability of the data in the equatorial regions may indicate that the modifying processes in the equatorial regions were not sufficient to erode and modify all the craters compared to the northernmost regions. Or, the presence of volatiles at the surface regions of higher latitudes makes the surface weaker during the modification stage of crater formation, emphasizing the infilling during the formation process.

It is important to highlight that these differences in the morphometric data could be due to differences in the spatial resolution of the images used to construct the DEM.

The spatial resolution between regions where the craters were collected varies between 80 and 300 m/pixel, while the vertical accuracy varies between 100 and 800 m [11]. A comparison made by Schenk [22] of Mercurian crater depths in images with spatial resolutions from 0.2 to ~1 km/pixel indicated little significant loss of depth information at these resolutions. As the resolution between the images used to obtain the crater data presented here varies by approximately 400 m/pixel, contemplating a variation significantly less than that tested by Schenk [22], the difference in the morphometric data in the different Pluto resolution zones [7,16] should not statistically influence the comparison of data. In addition, there is a group of craters within areas 1 and 2 that are in the same resolution zone, further demonstrating that it should not be the resolution that is influencing the difference in the morphometric data. So, we can assume two hypotheses: that our data will be little affected by the difference in resolution or, otherwise, that the DEM generated by stereogrammetry behaves differently from the photogrammetry data used by Schenk [22].

5. Conclusions

We have reported on the analysis of differences in morphometric characteristics throughout Pluto's surface for a globally and locally distributed population of craters. We have conducted a detailed study of crater morphometry using craters in the range from 5 to 60 km of diameter.

We have found that craters within areas 1 and 4 exhibit a simple to complex diameter transition (Dt) of ~10 km and craters within areas 3 and 5 exhibit a Dt of ~15 km. This difference suggests that there are some possible compositional differences throughout Pluto's crust. Since the transition diameter found in this work is higher than expected by the extrapolation from other icy bodies, we can assume that the crust of Pluto contains a higher percentage of rocky material than the Galilean satellites [10]. We also observed that craters within areas 1 and 2 are shallower than in other regions. This could be due to the presence of volatiles (mainly CH₄ and N₂) in those regions, that could influence crater morphology during its formation or during the volatile sublimation cycles. Equatorial craters have a higher range of depth values for a given diameter. This could be related to less intense modification processes in the equatorial regions, that were incapable of modifying all the craters. Craters larger than 20 km tend to exhibit smaller slopes of inner walls and higher data spread. This could be due to a modification process that affects mainly larger craters, such as ice relaxation.

The results presented here provide new insights on the relationships between morphometric parameters and terrain dependence, offering constraints for modeling landscape evolution and crater formation. Future works encompassing a detailed geological map of Pluto will contribute to understanding the dynamics of impact cratering on Pluto and provide further supporting evidence for the morphometric characterization of Pluto's surface.

In summary, the conclusions attained in this work are:

1. The transition from simple to complex craters in Pluto varies between 10 km (areas 1 and 4) and 15 km diameter (areas 3 and 5). This indicates that the dynamics of impact crater formation on Pluto is between the ones of icy and rocky bodies and do not follow the trend of icy bodies as expected from the inverse-gravity relationship.
2. Low slopes of inner walls and a high spread of data for craters greater than 20 km in diameter may indicate a modification process that has affected mainly larger craters.
3. Equatorial craters have a higher range of depth values for a given diameter. This could be related to less intense modification processes presented in the equatorial regions in modifying all the craters.
4. Differences in morphometry in each area could be related to different rheological properties of the target materials, explained by a higher proportion of rocky material in relation to other materials (ice) in area 3 and 5, as well as the presence of volatiles in area 1 and 2,

5. Volatile elements could be responsible for the incidence of shallower craters in the northern and northwestern regions. Volatile ices could influence crater formation and/or modify craters during Pluto's different seasons.

Supplementary Materials: The following materials are available online at <https://www.mdpi.com/2072-4292/13/3/377/s1>; Figure S1: Flowchart summarizing the Python code logic; Table S1: Complete data; Appendix S1: Python Code; Complete Python code available online at: <https://github.com/caiovnv/Impact-crater-morphometry>.

Author Contributions: Conceptualization, A.P.C. and C.V.N.V.; methodology, A.P.C., C.V.N.V., and C.H.G.; software, C.V.N.V.; formal analysis: C.V.N.V.; writing—original draft preparation, C.V.N.V.; writing—review and editing, C.V.N.V., A.P.C., and C.H.G.; supervision, A.P.C. and C.H.G. All authors have read and agreed to the published version of the manuscript.

Funding: We would like to acknowledge the first author's scholarship and financial aid provided by The São Paulo Research Foundation (FAPESP), grant #2018/22724-4. APC and CHG acknowledge their CNPq research grants 302679-2018-9 and 304413-2018-6, respectively. This study was partially funded by CAPES Brasil-Finance Code 001.

Institutional Review Board Statement: Not applicable.

Informed Consent Statement: Not applicable.

Data Availability Statement: The data used in this study are available in the supplementary material.

Acknowledgments: The authors are thankful to the Editor-in-Chief and the editors of this special issue, and the anonymous reviewers for their criticism and suggestions, which helped to improve the original manuscript.

Conflicts of Interest: The authors declare no conflict of interest. The funding institutions had no role in the design of the study, in the collection, analysis, or interpretation of the data, in the writing of the manuscript or in the decision to publish the results.

References

1. Susorney, H.C.; Barnouin, O.; Ernst, C.M.; Johnson, C.L. Morphometry of impact craters on Mercury from MESSENGER altimetry and imaging. *Icarus* **2016**, *271*, 180–193. [[CrossRef](#)]
2. Mangold, N.; Adeli, S.; Conway, S.; Ansan, V.; Langlais, B. A chronology of early Mars climatic evolution from impact crater degradation. *J. Geophys. Res. Space Phys.* **2012**, *117*. [[CrossRef](#)]
3. Robbins, S.J.; Watters, W.A.; Chappelow, J.E.; Bray, V.J.; Daubar, I.J.; Craddock, R.A.; Beyer, R.A.; Landis, M.E.; Ostrach, L.R.; Tornabene, L.; et al. Measuring impact crater depth throughout the solar system. *Meteorit. Planet. Sci.* **2017**, *53*, 583–637. [[CrossRef](#)]
4. Robbins, S.J.; Hynes, B.M. A new global database of Mars impact craters ≥ 1 km: 2. Global crater properties and regional variations of the simple-to-complex transition diameter. *J. Geophys. Res. Space Phys.* **2012**, *117*. [[CrossRef](#)]
5. Melosh, H.J. *Impact Cratering: A Geologic Process*; Oxford University Press: New York, NY, USA, 1989.
6. Watters, W.A.; Geiger, L.M.; Fendrock, M.; Gibson, R. Morphometry of small recent impact craters on Mars: Size and terrain dependence, short-term modification. *J. Geophys. Res. Planets* **2015**, *120*, 226–254. [[CrossRef](#)]
7. Singer, K.N.; McKinnon, W.B.; Gladman, B.; Greenstreet, S.; Bierhaus, E.B.; Stern, S.A.; Parker, A.H.; Robbins, S.J.; Schenk, P.; Grundy, W.; et al. Impact craters on Pluto and Charon indicate a deficit of small Kuiper belt objects. *Science* **2019**, *363*, 955–959. [[CrossRef](#)] [[PubMed](#)]
8. Moore, J.M.; McKinnon, W.; Spencer, J.R.; Howard, A.D.; Schenk, P.; Beyer, R.A.; Nimmo, F.; Singer, K.N.; Umurhan, O.M.; White, O.L.; et al. The geology of Pluto and Charon through the eyes of New Horizons. *Science* **2016**, *351*, 1284–1293. [[CrossRef](#)] [[PubMed](#)]
9. Robbins, S.J.; Singer, K.N.; Bray, V.J.; Schenk, P.; Lauer, T.R.; Weaver, H.A.; Runyon, K.; McKinnon, W.; Beyer, R.A.; Porter, S.B.; et al. Craters of the Pluto-Charon system. *Icarus* **2017**, *287*, 187–206. [[CrossRef](#)]
10. Robbins, S.J.; Schenk, P.M.; Riggs, J.D.; Parker, A.H.; Bray, V.J.; Beddingfield, C.B.; Beyer, R.A.; Verbiscer, A.J.; Binzel, R.; Runyon, K.D. Depths of Pluto's and Charon's craters, and their simple-to-complex transition. *Icarus* **2021**, *356*, 113902. [[CrossRef](#)]
11. Schenk, P.; Beyer, R.A.; McKinnon, W.B.; Moore, J.M.; Spencer, J.R.; White, O.L.; Singer, K.; Umurhan, O.M.; Nimmo, F.; Lauer, T.R.; et al. Breaking up is hard to do: Global cartography and topography of Pluto's mid-sized icy Moon Charon from New Horizons. *Icarus* **2018**, *315*, 124–145. [[CrossRef](#)]
12. Grundy, W.; Binzel, R.; Buratti, B.; Cook, J.C.; Cruikshank, D.P.; Ore, C.M.D.; Earle, A.M.; Ennico, K.; Howett, C.; Lunsford, A.W.; et al. Surface compositions across Pluto and Charon. *Science* **2016**, *351*, aad9189. [[CrossRef](#)] [[PubMed](#)]

13. Geiger, L.M. Statistical Analysis of Simple Martian Impact Crater Morphometry. Honors Thesis, Wellesley College Digital Collections, Wellesley, MA, USA, 2013.
14. QGIS Development Team; QGIS Geographic Information System. Open Source Geospatial Foundation Project. 2020. Available online: <http://qgis.osgeo.org> (accessed on 10 December 2020).
15. Bray, V.J.; Schenk, P.M. Pristine impact crater morphology on Pluto—Expectations for New Horizons. *Icarus* **2015**, *246*, 156–164. [[CrossRef](#)]
16. Schenk, P.M.; Singer, K.N.; Robbins, S.J.; Bray, V.J.; Beyer, R.A.; Moore, J.M.; McKinnon, W.B.; Spencer, J.R.; Runyon, K.; Stern, S.A.; et al. Topography of Pluto and Charon: Impact Cratering. In Proceedings of the 47th Lunar and Planetary Science Conference, The Woodlands, TX, USA, 21–25 March 2016; p. 2795.
17. O’Keefe, J.D.; Ahrens, T.J. Planetary cratering mechanics. *J. Geophys. Res. Space Phys.* **1993**, *98*, 17011–17028. [[CrossRef](#)]
18. Zahnle, K.; Schenk, P.; Levison, H.; Dones, L. Cratering rates in the outer Solar System. *Icarus* **2003**, *163*, 263–289. [[CrossRef](#)]
19. Schenk, P. Thickness constraints on the icy shells of the galilean satellites from a comparison of crater shapes. *Nat. Cell Biol.* **2002**, *417*, 419–421. [[CrossRef](#)] [[PubMed](#)]
20. Schenk, P.; Zahnle, K. On the negligible surface age of Triton. *Icarus* **2007**, *192*, 135–149. [[CrossRef](#)]
21. White, O.L.; Schenk, P.M.; Bellagamba, A.W.; Grimm, A.M.; Dombard, A.J.; Bray, V.J. Impact crater relaxation on Dione and Tethys and relation to past heat flow. *Icarus* **2017**, *288*, 37–52. [[CrossRef](#)]
22. Schenk, P.M. Crater formation and modification on the icy satellites of Uranus and Saturn: Depth/diameter and central peak occurrence. *J. Geophys. Res. Space Phys.* **1989**, *94*, 3813–3832. [[CrossRef](#)]
23. Trowbridge, A.J.; Melosh, H.J.; Freed, A.M. Impacts into Pluto: The Effect of a Nitrogen Ice Surface Layer. In Proceedings of the Bridging the Gap III: Impact Cratering in Nature, Experiments, and Modeling, University of Freiburg, Freiburg, Germany, 21–26 September 2015; p. 1091.